

THERMALS IN STRATIFIED REGIONS OF THE ISM

A. Rodríguez-González & A. C. Raga

Instituto de Ciencias Nucleares, UNAM, México

Received: November 7, 2018; Accepted: Year Month Day

RESUMEN

Presentamos un modelo de una burbuja caliente que flota dentro de una región del medio interestelar con estratificación exponencial. Este modelo incluye términos representando el frenado debido a la presión hidrodinámica y debido a la incorporación de masa ambiental a la burbuja. Calibramos los parámetros libres asociados con estos dos términos mediante una comparación con simulaciones tridimensionales de una burbuja que flota. Finalmente, aplicamos nuestro modelo al caso de una burbuja caliente producida por una supernova que explota dentro del medio interestelar estratificado de la galaxia.

ABSTRACT

We present a model of a “thermal” (i.e., a hot bubble) rising within an exponentially stratified region of the ISM. This model includes terms representing the ram pressure braking and the entrainment of environmental gas into the thermal. We then calibrate the free parameters associated with these two terms through a comparison with 3D numerical simulations of a rising bubble. Finally, we apply our “thermal” model to the case of a hot bubble produced by a SN within the stratified ISM of the Galactic disk.

Key Words: GALAXIES: HALOS – ISM: CLOUDS – STARS: FORMATION

1. INTRODUCTION

There are two simple models for buoyant flows in the Earth’s atmosphere:

- plumes: continuous flows produced by a heat source in the base of the atmosphere,
- thermals: rising bubbles resulting from an instantaneous release of hot air.

These flows are described in detail, e.g., in the classic book of Turner (1980).

Plumes have received considerable attention in the ISM literature, having normally been called “nozzles” (Blandford & Rees 1974). These nozzle flows resemble atmospheric plumes, but are fully compressible (plumes in the Earth’s atmosphere being in a highly subsonic, anelastic regime), as discussed by Rodríguez-González et al. (2009).

Less attention has been devoted to “thermals”. Mathews et al. (2003) and Nusser et al. (2006) develop “hot bubble” models for buoyant regions within cooling flows in clusters of galaxies, including the effects of the buoyancy and

the “ram pressure braking” of the bubble as it moves within the surrounding environment.

Interestingly, both the astrophysical “plume” (nozzle) and “thermal” (“hot bubble”) models do not include terms representing the entrainment of environmental material into the buoyant flow. Actually, Pope et al. (2010) do discuss the possible importance of such a term, and evaluate its effects on the dynamics of a rising hot bubble. This situation is somewhat curious, since it is clear that the entrainment term is fundamental for the development of buoyant flows in Earth’s atmosphere.

In the present paper, we develop a model for a fully compressible (as opposed to anelastic) “thermal” (i.e., a positively buoyant “hot bubble”) rising in an exponentially stratified atmosphere, which includes terms representing the effects of “ram pressure braking” and “entrainment”. Both of these terms lead to a slowing down of the motion of the bubble through the environment (section 2). We then compare this model with 3D numerical simulations of a buoyant bubble, and show that both the ram pressure braking and the entrainment terms are necessary in order to obtain a good agreement of the “thermal” model with the numerical simulations (section 3).

Using the entrainment and ram pressure braking terms calibrated with the numerical simulations, we then explore the full parameter space of the “thermal in an exponentially stratified atmosphere” problem (section 4). Also, we explore an application of this model to the case of the hot bubble produced by a supernova exploding within the ISM of the Galactic plane (section 5). Finally, the results are summarized in section 6.

2. THE COMPRESSIBLE THERMAL MODEL

Let us consider a model of a hot bubble immersed in a cooler, stratified environment with a pressure stratification $P_a(z)$ given by the hydrostatic condition:

$$\frac{dP_a}{dz} = -\rho_a g, \quad (1)$$

where $\rho_a(z)$ is the ambient density stratification and g is the gravitational acceleration.

The pressure+gravitational force per unit volume on a parcel of density ρ in pressure balance with the pressure P_a of the surrounding environment then is:

$$f_z = -\frac{dP_a}{dz} - \rho g = (\rho_a - \rho) g, \quad (2)$$

where for the second equality we have used equation (1).

We now write the equations for the time evolution of the ascending parcel:

$$\frac{dM}{dt} = \rho_a v_e A, \quad (3)$$

where $M = \rho V$ (with ρ the average density and V the volume of the parcel) is the mass of the parcel, A is its surface area and v_e the so-called “entrainment

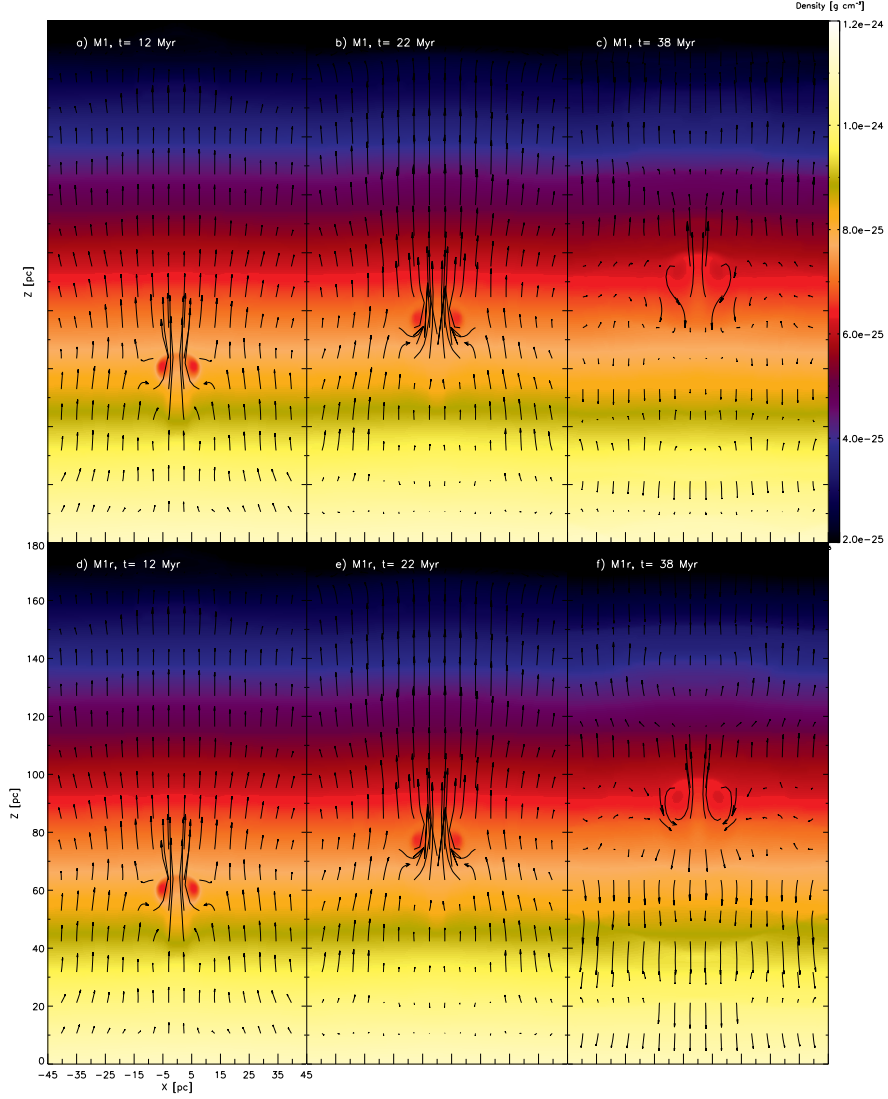


Fig. 1. Density stratifications on the mid xz -plane of the 3D simulations of a rising bubble, obtained from models M1 (top) and M1r (bottom frames). The initially spherical, hot bubble is centered at $z_0 = 35$ pc, and the bubble then rises in the stratified environment developing a “ring vortex” structure. This vortical structure is traced by the flow velocity (shown with the arrows). Three frames are shown, corresponding to $t = 12$ Myr (left), 22 Myr (centre) and 38 Myr (right) frames. The bar on the top right gives the density colour scale in g cm^{-3} . From the displayed stratifications it is clear that appreciable differences between the non-radiative (M1, top frames) and radiative model (M1r, bottom frames) only appear at later evolutionary times (i.e., for $t = 38$ Myr).

velocity” associated with the flux of ambient material incorporated into the

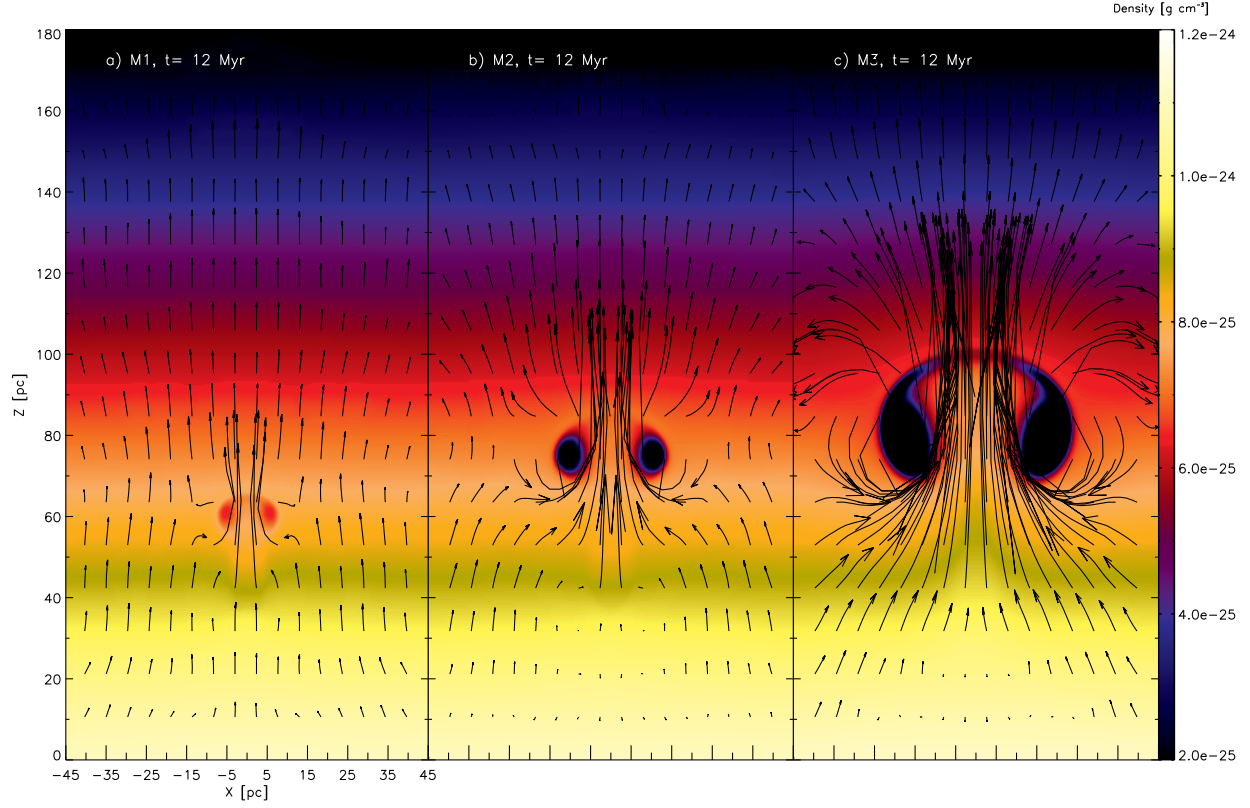


Fig. 2. Density stratifications and velocity fields on the mid xz -plane of the 3D simulations of a rising bubble, obtained from models M1, M2 and M3 for a $t = 12$ Myr evolutionary time. The bar on the right gives the density colour scale in g cm^{-3} .

volume of the ascending parcel. The momentum equation is:

$$\frac{d\Pi}{dt} = (\rho_a - \rho) gV - \rho_a u |u| A_c, \quad (4)$$

where $\Pi = Mu = \rho V u$ (with u being the z -velocity) is the momentum of the parcel along the z -axis. The second term on the right hand side of this equation represents the drag due to the ram pressure of the environment which is pushed aside by the thermal, which presents an effective area A_c . This term is negligible in the highly subsonic case, but becomes important for mildly subsonic flows.

Finally, the energy equation can be written as:

$$\frac{dE}{dt} = -P_a \frac{dV}{dt} + \frac{P_a}{\gamma - 1} v_e A, \quad (5)$$

where $E = PV/(\gamma - 1)$ is the thermal energy of the parcel (assumed to be in local pressure equilibrium with the surrounding environment) and $P_a/(\gamma - 1)$

is the ambient thermal energy per unit volume. As usual, γ is the specific heat ratio (which we assume has the same value for the parcel and for the ambient medium). In this energy equation, we have assumed that the cooling due to entrainment (second term in the right of equation 5) dominates over the radiative cooling of the rising bubble.

We now close the system of equations (3-5) assuming that the ascending parcel has a homologous expansion (maintaining the same shape) and that the entrainment velocity is proportional to the velocity of the parcel, so that

$$A = V^{2/3}; \quad v_e = \alpha|u|, \quad (6)$$

where the numerical factor in the A/V relation is absorbed into the α parameter (assumed to be constant) of the second relation (as A and v_e always appear as the product Av_e , see equations 3 and 5). We also write the effective area A_c with which the thermal pushes away the environmental gas as:

$$A_c = \beta V^{2/3}, \quad (7)$$

where β is a constant of order unity.

With the relations of (6-7), equations (3-5) can then be written as:

$$\text{mass:} \quad \frac{dM}{dt} = \alpha \rho_a |u| V^{2/3}; \quad M = \rho V, \quad (8)$$

$$\begin{aligned} \text{momentum:} \quad \frac{d\Pi}{dt} &= (\rho_a - \rho) g V - \beta \rho_a u |u| V^{2/3}; \\ \Pi &= \rho V u, \end{aligned} \quad (9)$$

$$\text{entropy:} \quad \frac{dS}{dt} = \alpha P_a |u| V^{\gamma-1/3}; \quad S = P_a V^\gamma, \quad (10)$$

where some simple manipulation has been made to convert (5) into an entropy conservation form.

Finally, we specify a simple, plane, isothermal atmosphere environmental stratification

$$\rho_a(z) = \rho_0 e^{-z/H}; \quad \text{with } H = \frac{c_a^2}{g}, \quad (11)$$

which is the solution to equation (1) for constant g . The environmental pressure $P_a(z) = c_a^2 \rho_a(z)$ (where c_a is the environmental isothermal sound speed) follows the same exponential law.

Equations (8-11) can be integrated analytically only in a partial way (see Appendix A). We therefore integrate numerically equations (8-10) to obtain $V(t)$, $\rho(t)$, $u(t)$ and its time-integral $z(t)$, for an exponential environmental density/pressure stratification (with an isothermal sound speed c_a and a gravitational acceleration g , see equation 11). As initial conditions (at $t = 0$) we set $z = 0$, $u = 0$ and choose an initial volume V_0 and density ratio ρ_c/ρ_0 between the initial clump density and the $z = 0$ environmental density.

It is of course necessary to specify the two free parameters α and β (see equations 6 and 7). As we have stated above, one expects to have $\beta \sim$

1. Also, in order to reproduce laboratory experiments of thermals it is well known that one needs to choose $\alpha \sim 0.1$. In the following section we present 3D simulations of a thermal in an exponential atmosphere. We then use a comparison of the resulting $z(t)$ dependencies with an integration of equations (8-10) to determine the α and β parameters.

3. NUMERICAL SIMULATIONS

In order to see whether or not the model presented in section 2 does reproduce the features of a hot bubble rising in a stratified atmosphere, we have computed 3D simulations of the flow. This has been done with a 3D version of the “yguazú-a” code (Raga et al. 2000), using a 4-level adaptive grid with a maximum resolution of 0.352 pc along the three axes. The domain has an extent of (90, 90, 180) pc along the (x, y, z) -axes, with reflection conditions on the $\pm z$ boundaries and transmission conditions in all of the other boundaries.

The equations for a $\gamma = 5/3$ gas are integrated, considering a gravitational force in the $-z$ -direction (with constant g , included in the momentum and energy equations). We have computed non-radiative simulations, and simulations including the parametrized radiative energy loss term of Raga & Reipurth (2004), with a low temperature cutoff at 10^4 K. The domain is initially filled with an isothermal, stratified density structure $n_a = n_0 \exp[-(z - z_0)/H]$ with $n_0 = 1 \text{ cm}^{-3}$, $H = 150 \text{ pc}$ and $z_0 = 35 \text{ pc}$. This environment has a temperature of 10^4 K (corresponding to an isothermal sound speed $c_a = 11.8 \text{ km s}^{-1}$). The corresponding value of g is then computed as $g = c_a^2/H$.

The hot bubble is initially spherical, located in the centre of the xy range of the computational domain, and at a height $z_0 = 35 \text{ pc}$ from the bottom of the z -axis. The bubble has an initial density $n_c = 0.01 \text{ cm}^{-3}$ and temperature $T_c = 10^6 \text{ K}$, so that it is in pressure equilibrium with the environment at a height z_0 . We have computed non-radiative and radiative models using the three values of the initial radius R_0 of the bubble which are given in Table 1.

Starting with this initial condition, the 3D Euler equations are integrated forward in time, following the rise of the positively buoyant bubble and its eventual mixing with the environment. Three frames of the resulting time evolution of models M1 (non-radiative) and M1r (radiative, see Table 1) are shown in Figure 1.

At a time $t = 12 \text{ Myr}$ (left frames of Figure 1), the bubble has risen to a height $z \approx 50 \text{ pc}$, and has developed a vortical structure, which is maintained throughout the evolution of the flow. At $t = 22 \text{ Myr}$, the bubble has risen to a height $z \approx 65 \text{ pc}$, and the vortex ring has expanded sideways quite considerably. At $t = 38 \text{ Myr}$ (right frames of Figure 1), the rise of the vortex has slowed down quite considerably, reaching a maximum height of $\approx 95 \text{ pc}$. At longer times the vortex slowly drops to $z \sim 90 \text{ pc}$, while mixing heavily with the environment, and rapidly becoming unrecognizable as a coherent structure.

From Figure 1, we see that the non-radiative (M1, top) and radiative (M1r, bottom) simulations only show appreciable differences at the later, $t = 38$ Myr evolutionary time. Approximately the same maximum height is attained by the thermal in the radiative and in the non-radiative models.

Figure 2 shows the mid-plane density stratifications and flow fields at $t = 12$ Myr obtained from our 3 non-radiative models (M1, M2 and M3), illustrating the flow configurations obtained for the three chosen initial radii of the thermal (see Table 1). At this integration time, the flows obtained from the corresponding radiative simulations (models M1r, M2r and M3r) are basically identical to the corresponding non-radiative flows.

From the simulations, we can determine the height $z - z_0$ (where z_0 is the height of the initial, hot bubble) as a function of time t . We associate the (time-dependent) height of the ascending thermal with the position at which the vertical velocity has its maximum value, which approximately corresponds to the centre of the rising vortex ring. The resulting height vs. time dependencies obtained from our six simulations are shown in Figure 3.

We then compute “thermal” models (see section 2) with an initial bubble to environment density ratio $\rho_c/\rho_0 = 0.01$, and with an initial volume $V_0 = 4\pi R_0^3$ (corresponding to the parameters of the numerical simulations, see above and Table 1), and with arbitrary values of the dimensionless parameters α and β (see equations 6 and 7). Through least squares fits to the (appropriately adimensionalized) position of the rising vortex in the 3D simulations, we obtain the best fit thermal models, shown with solid lines in the three frames of Figure 3. The values of α and β obtained from fits to the three non-radiative models are given in the two last columns of Table 1 (very similar numbers being obtained from fits to the non-radiative models).

In order to show that it is actually necessary to have non-zero α and β values, we have also carried out least squares fits to model M2 setting $\alpha = 0$ (from which we obtain $\beta = 1.91$) and $\beta = 0$ (from which we obtain $\alpha = 0.27$). These best fits (shown with the dashed lines in the central frame of Figure 3) fail to reproduce the $z(t)$ dependence obtained from the M2 numerical simulation in a satisfactory way.

From this comparison, we conclude that in order to reproduce the rise of the hot bubble obtained from the numerical simulation, the quasi-analytic “thermal” model needs to have both the “entrainment” and the “ram pressure braking” terms included in equations (8-10). The dimensionless parameters (associated with these two terms) deduced from fits to the numerical simulations are $\alpha \approx 0.2$ and $\beta \approx 0.7$, which correspond to the average of the three values obtained by fitting models M1, M2 and M3 (see Table 1).

Needless to say, the numerical simulations which we are using have a limited spatial resolution, and the values deduced for α and β will probably differ when changing the resolution of the simulation. However, the fact that these two parameters are consistent with their expected values indicates that the results that we obtained are approximately correct.

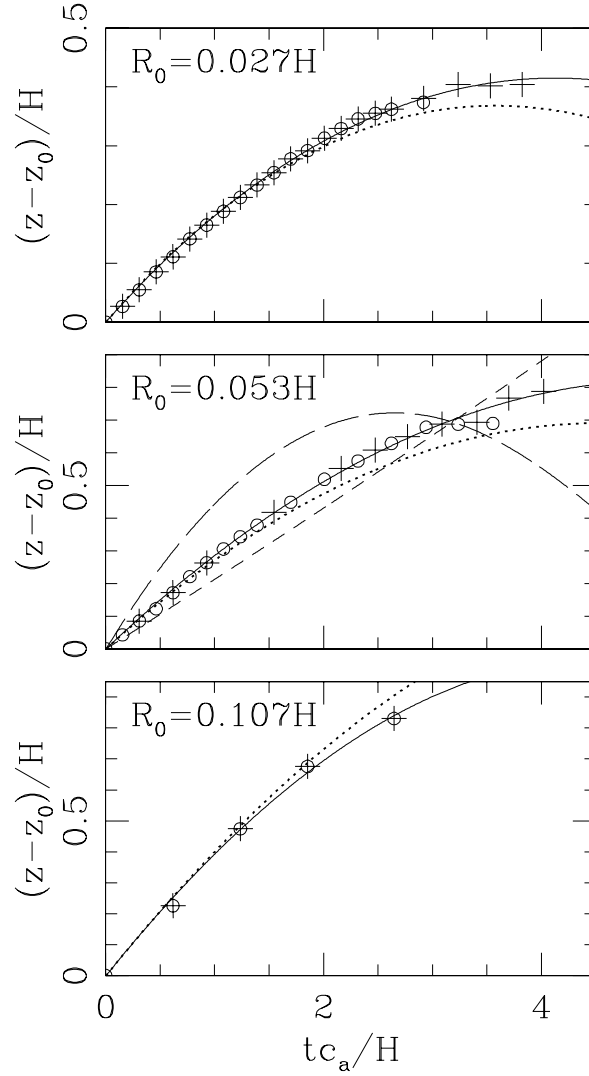


Fig. 3. Height of the hot bubble obtained from the numerical simulations as a function of time (crosses: non-radiative models, open circles: radiative models) and fits to these time dependencies with “thermal” models (solid, dashed and dotted lines). The top frame shows models M1 and M1r, the central frame models M2 and M2r and the bottom frame models M3 and M3r. The solid lines correspond to thermal models with the α and β parameters corresponding to least squares fits to the z vs. t dependencies obtained from the three non-radiative simulations. The dotted lines correspond to a thermal model with $\alpha = 0.2$ and $\beta = 0.7$ (the average of the values obtained for the 3 non-radiative models, see Table 1). In the central frame, we have included the z vs. t dependencies obtained from best fit $\alpha = 0$ (short dashes) and $\beta = 0$ (long dashes) thermal models, illustrating the fact that in order to reproduce the simulations it is necessary to include both the entrainment and the ram pressure braking terms.

TABLE 1
RADIAL COLLAPSE MODELS

Model ^(a)	R_0 ^(b)	R_0/H ^(c)	α ^(d)	β ^(e)
M1, M1r	4 pc	0.027	0.181	0.774
M2, M2r	8 pc	0.053	0.169	0.678
M3, M3r	16 pc	0.107	0.278	0.606

^amodels M1-3 are non-radiative and models M1r-3r are radiative

^binitial radius R_0 of the bubble

^c R_0 in units of the environmental scaleheight

^d“entrainment” parameter

^e“ram pressure braking” parameter

4. EXPLORATION OF THE PARAMETER SPACE

We now consider the “rising thermal” model (see section 2) with the $\alpha = 0.2$ (entrainment) and $\beta = 0.7$ (ram pressure drag) parameters deduced from the comparison with 3D numerical simulations (see section 3). If we write the height z in units of the environmental scale height H , the vertical velocity u in terms of the environmental isothermal sound speed c_a and the time t in units of H/c_a , the problem has two free parameters: the initial volume V_0 (in units of H^3) and the initial clump to environment density ratio ρ_c/ρ_0 .

Integrating numerically Equations (8-10), we have computed three “thermal” models with $\rho_c/\rho_0 = 0.1$ and $V_0 = 0.02, 0.1$ and $0.5 H^3$. The resulting dimensionless height z/H and vertical velocity u/c_a are plotted as a function of time $t c_a/H$ in Figure 4. It is clear that for increasing values of V_0 the rising thermal reaches a larger maximum height, before falling again following a damped, oscillatory behaviour.

As we have shown in section 2, 3D numerical simulations produce a rise which is similar to the one predicted by the quasi-analytic “thermal” model. However, once the maximum height is reached the rising vortex obtained in the numerical simulations expands laterally and mixes heavily with the environment, and only shows a small drop in height from its maximum. Therefore, the oscillatory behaviour obtained at larger times from the single-parcel “thermal” model does not correspond to a real physical phenomenon. Applications of the rising “thermal” model therefore have to be limited to the initial rise of the hot bubble.

We have then computed a matrix of “thermal” models with $0 < \rho_c/\rho_0 \leq 0.5$ and $0 < V_0 \leq 0.5 H^3$. From these models we have computed the maximum height z_{max} reached by the rising thermal. The resulting values of z_{max} as a function of ρ_c/ρ_0 and V_0 are shown in Figure 5.

From this Figure, it is clear that for $V_0 > 0.02 H^3$ one has $z_{max} > H$ for all of the explored values of $0 < \rho_c/\rho_0 \leq 0.5$. In order for the thermal to reach $z_{max} \sim 3 H$, one needs to have low ρ_c/ρ_0 values (~ 0.1) and high values of V_0

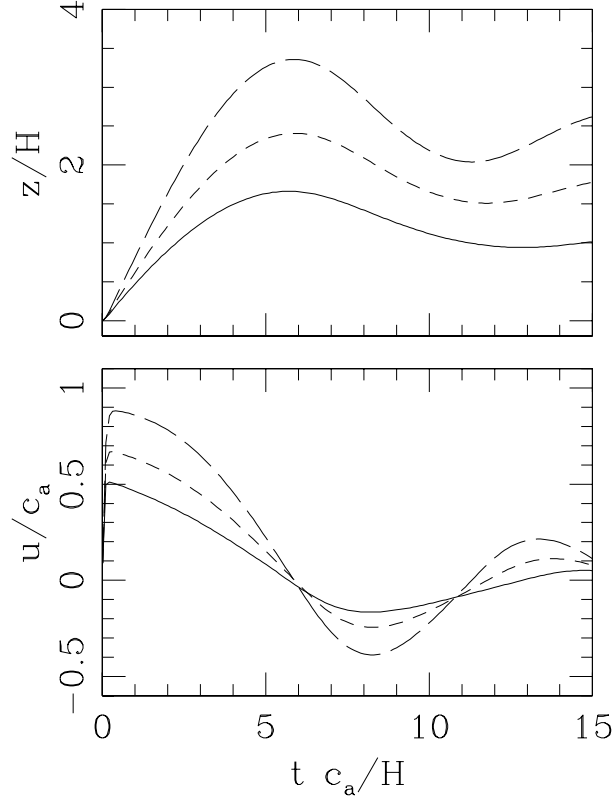


Fig. 4. Thermal model with $\alpha = 0.2$, $\beta = 0.7$, $\rho_c/\rho_0 = 0.1$ and $V_0 = 0.02 H^3$ (solid lines), $0.1 H^3$ (short dashes) and $0.5 H^3$ (long dashes). The height of the thermal as a function of time is shown on the top frame, and its velocity in the bottom frame.

($\sim 0.3 H^3$), corresponding to the lower, right hand region of Figure 5.

5. A SUPERNOVA BUBBLE WITHIN THE WARM ISM

This model can be applied to the case of a supernova (SN) explosion embedded in a dense region of warm ($n \sim 10^3 \text{ cm}^{-3}$, $T \sim 10^3 \text{ K}$) gas in the plain of the Galaxy. Raga et al. (2012) have shown that the hot bubble produced by a SN explosion first expands and then reaches a maximum radius

$$R_f = \left[\frac{3(\gamma^2 - 1)}{8\pi\gamma} \frac{E}{\gamma\rho_0 c_a^2} \right]^{1/3}, \quad (12)$$

in a time

$$t_f = \frac{(\gamma + 1)R_f}{2\sqrt{\gamma}c_a}, \quad (13)$$

where ρ_0 is the density and c_a the (isothermal) sound speed of the uniform environment. At this evolutionary stage, the hot bubble is in approximate pressure equilibrium with the surrounding environment.

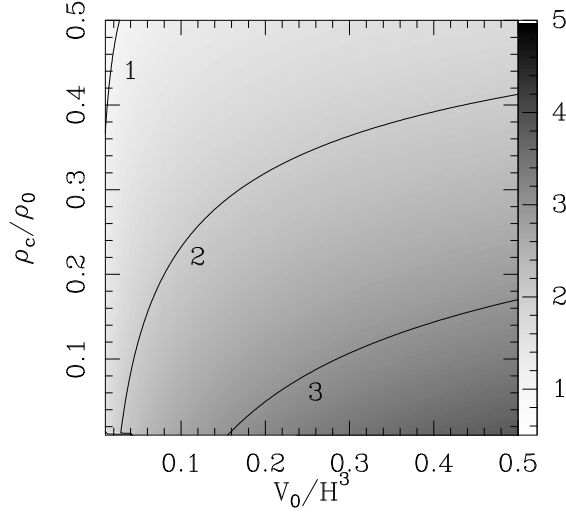


Fig. 5. Maximum height z_{max} attained by the thermal as a function of its initial volume V_0/H^3 (with H being the environmental scale height) and its initial clump to environmental density ratio ρ_c/ρ_0 . The labeled contours correspond to $z_{max}/H = 1, 2$ and 3 .

Let us now consider a SN explosion within a warm ISM region of number density $n_0 = 1 \text{ cm}^{-3}$ and sound speed $c_a = 10 \text{ km s}^{-1}$. For a SN energy $E = 10^{50} \text{ erg}$, from equations (12-13) we then obtain $R_f \approx 81 \text{ pc}$ and $t_f \approx 8.2 \times 10^6 \text{ yr}$. The temperature of this hot bubble is much larger than the one of the cloud, so that the bubble to environment density ratio will have a value $\rho_c/\rho_0 \ll 1$.

As the warm ISM in the Galaxy has a scale height $H \approx 150 \text{ pc}$, the SN bubble has an initial radius $R_f \approx 0.54 H$, and therefore an initial volume $V_c = 4\pi R_f^3/3 \approx 0.66 H^3$. We then compute a “thermal” model with this value of V_c and with $\rho_c/\rho_0 = 10^{-2}$ (the actual value of this ratio being unimportant provided that it is $\ll 1$). The results from this model are shown in Figure 5.

From this Figure, we see that the initial bubble rises at a transonic velocity of $\sim 10 \text{ km s}^{-1}$ and then slows down, reaching a maximum height $z_{max} \approx 600 \text{ pc}$ (of 4 environmental scale heights) at a time $t \approx 90 \text{ Myr}$. Therefore, before reaching this point in reality the rising bubble will emerge from the stratified ISM of the Galactic disk into the hot ISM of the halo.

6. SUMMARY

This paper describes a quasi-analytic “rising thermal” model: a compressible, single parcel model including “entrainment” and a “ram pressure braking” terms. This model differs from “thermal” models from the atmospheric sciences in that it is fully compressible (atmospheric thermals being approximately anelastic) and in the presence of the ram pressure braking term. This term is active in the transonic regime relevant for astrophysical thermals, but

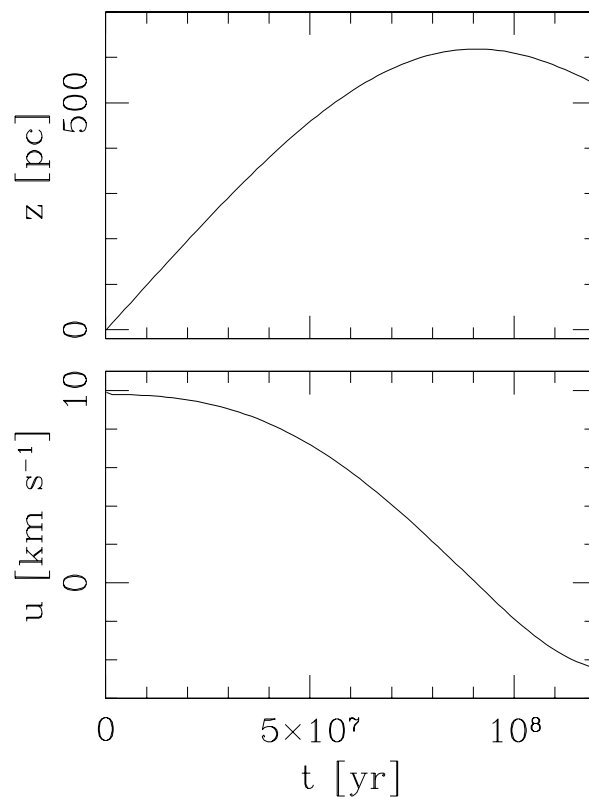


Fig. 6. Dimensional height (top) and velocity (bottom) for the model of a SN bubble rising in the stratified, warm ISM of the Galactic plane (see section 5).

is not important in the highly subsonic, atmospheric case. We limit our study to the case of a thermal in an exponentially stratified, isothermal atmosphere.

The model (see section 2) has two free dimensionless parameters: α , associated with the entrainment term and β , associated with the ram pressure braking term (see equations 6-7). From fits to 3D numerical simulations (see section 3), we find estimates $\alpha = 0.2$ and $\beta = 0.7$ for these two parameters. We find that the two terms (ram pressure braking and entrainment) are necessary for reproducing the results obtained from the numerical simulation.

With these α and β parameters, we then compute a grid of models varying the initial parameters V_0/H^3 (the ratio between the initial volume of the hot bubble and the cube of the environmental scale height) and ρ_c/ρ_0 (the initial ratio between the densities of the bubble and of the surrounding environment), obtaining the maximum height z_{max} attained by the rising thermal (see section 4). We find that for $V_0/H^3 \sim 0.4$, one has thermals that rise several scale environmental heights.

Finally, as a possible application of our model, we describe the case of a SN explosion within the warm ISM of the Galactic disk (section 5). We consider the hot bubble produced by an $E = 10^{50}$ erg SN within an environment of

density $n_0 = 1 \text{ cm}^{-3}$ and sound speed $c_a = 10 \text{ km s}^{-1}$, with a scale height $H = 150 \text{ pc}$. We show that the SN bubble takes $\sim 8 \text{ Myr}$ to reach a pressure equilibrium radius $R_f \sim 80 \text{ pc}$ ($\approx 0.5 H$). Over a longer timescale, this hot bubble rises in the stratified ISM of the Galactic disk, reaching a height of $\sim 600 \text{ pc}$ in $\sim 90 \text{ Myr}$. The bubble will therefore leave the disk ISM, and enter the hot ISM associated with the Galactic halo.

Such rising thermals might be important for feeding the turbulence of the Galactic ISM, and the models presented in this paper would provide a clear guide for the future calculation of numerical simulations of this process. Our present model could possibly also be applied to other transient flows in the ISM in which buoyancy plays an important effect. An example of such flows is of course the dynamics of buoyant bubbles within cooling flows (see Pope et al. 2010 and references therein).

We acknowledge support from the CONACyT grants 61547, 101356, 101975, 165584, 167611 and 167625, and the DGAPA-UNAM grants IN105312 and IN106212.

APPENDIX A: PARTIAL ANALYTIC SOLUTION OF THE THERMAL MODEL

The system of equations (8-10) for a rising thermal can be integrated in a partial way. We start from the “entropy conservation” equation (10). Setting $P_a = c_a^2 \rho_a$, with ρ_a given by equation (11) and using the relation $d/dt = u dz/dz$, equation (10) can be written in the form:

$$\frac{d}{dz} \left(V^\gamma e^{-z/H} \right) = \alpha V^{\gamma-1/3} e^{-z/H}. \quad (14)$$

Now, setting $V^{\gamma-1/3} \approx V^\gamma / V_m^{1/3}$ (where V_m is the average volume of the rising parcel), equation (14) can be integrated to obtain:

$$V(z) = V_0 e^{z/H_1}; \text{ where } \frac{1}{H_1} = \frac{1}{\gamma} \left(\frac{1}{H} + \frac{\alpha}{V_m^{1/3}} \right). \quad (15)$$

One of course does not know the value of the average volume V_m . We find that if we set $V_m = 3V_0$ (where V_0 is the volume of the thermal at $z = 0$), equation (15) agrees with the exact (i.e., numerical) integration of equation (14) to within 4% in the $z = 0 \rightarrow 4H$ range.

We can then insert this $V(z)$ solution into equation (8), and straightforwardly integrate over z to obtain:

$$\rho(z) = \left[\rho_c - \frac{\alpha \rho_0 H_2}{V_0^{1/3}} \left(e^{-z/H_2} - 1 \right) \right] e^{-z/H_1}, \quad (16)$$

where $H_2^{-1} = H^{-1} - 2/(3H_1)$. Equation (16) agrees with the exact (numerical) integration of equations (8, 10) to within 2.5% in the $z = 0 \rightarrow 4H$ range.

We have not, however, found an exact or approximate integration of Equation (9), so as to obtain the vertical velocity u of the thermal as a function of z . Following the suggestion of Nusser et al. (2006), one can obtain an estimate of the flow velocity by assuming an approximate balance between the buoyancy and the drag terms (i.e., setting the right hand side of equation 9 to zero). From this condition, one finds u as a function of ρ , ρ_a and V . Through the previously determined dependencies of these variables on z one then finds $u(z)$.

However, we find that the vertical velocity $u(z)$ determined in this way agrees with the exact (numerical) integration of equation (9) only to an order of magnitude. Therefore, a reasonably accurate description of the rising thermal solution can only be obtained by using the analytic expressions for the volume $V(z)$ and the density $\rho(z)$ (equations 15 and 16) and then carrying out a numerical integration of equation (9) in order to obtain $u(z)$. The “thermal” solution as a function of t is then obtained by integrating the differential equation $dz/dt = u$.

REFERENCES

- Blandford, R. D., Rees, M. J. 1974, MNRAS, 169, 395
 Mathews, W. G., Brighenti, F., Buote, D. A., Lewis, A. D. 2003, ApJ, 596, 159
 Nusser, A., Silk, J., Babul, A. 2006, MNRAS, 373, 739
 Pope, E. C. D., Babul, A., Pavlovski, G., Bower, R. G., Dotter, A. 2010, MNRAS, 406, 2023
 Raga, A. C., Cantó, J., Rodríguez, L. F., Velázquez, P. F. 2012, MNRAS, 424, 2522
 Raga, A. C., Reipurth, B. 2004, RMxAA, 40, 15
 Raga, A. C., Navarro-González, R., Villagrán-Muniz, M., 2000, RMxAA, 36, 67
 Rodríguez-González, A., Raga, A. C., Cantó, J. 2009, A&A, 501, 411
 Turner, S. 1980, “Buoyancy effects in fluids”, Cambridge monographs on mechanics (Cambridge Univ. Press)

A. Rodríguez-González, A. C. Raga: Instituto de Ciencias Nucleares, Universidad Nacional Autónoma de México, Ap. 70-543, 04510 D. F., México (ary,raga@nucleares.unam.mx)